On the Comparison of Two Novel Interval Field Formulations for the Representation of Spatial Uncertainty

Maurice Imholz[1)], Matthias Faes[2)], Jasper Cerneels[2)], Dirk Vandepitte[1)] and David Moens[2)]
[1)] *KU Leuven - Department of Mechanical Engineering, Celestijnenlaan 300, B-3000 Leuven*
[2)] *KU Leuven - Department of Mechanical Engineering, Technology campus De Nayer, B-2860 St.-Katelijne-Waver*

Abstract: This paper concerns the comparison of two established interval field methods for the representation of spatially varying non-determinism in an FE model: Inverse Distance Weighting (IDW) interpolation and the Local Interval Field Decomposition (LIFD) method. The comparison is first made from a theoretical point of view, highlighting the advantages of both techniques as compared to each other. Next, both IDW and LIFD are applied to a dynamical model of a U-shaped hollow tube and the resulting uncertain regions at the output side of the model are compared qualitatively. It is shown that both techniques are complementary to each other due to the trade-off in their ability to represent the uncertainty set at the output side of the model and the involved computational cost.

Keywords: interval fields, uncertainty, non-deterministic modelling

1. Introduction

In the context of integrating uncertainty and variability in Finite Element (FE) models, several advanced techniques for taking both inter- (between nominally identical parts) and intra-variability (spatial variability within one part) into account have recently been introduced. In the framework of possibilistic non-determinism, especially the theory of Interval Fields (IF) has been proven to show promising results. Following this approach, variability in the input parameters of the FE model is introduced as the superposition of a number of base vectors scaled by interval factors. In the recent past, two techniques for the construction of interval fields have been introduced by the authors: Inverse Distance Weighting interpolation (IDW) and the Local Interval Field Decomposition method (LIFD). In this paper, these two established interval field methods are compared in their ability to represent different uncertain input sets and the computational work required. Both techniques are compared theoretically, as well as applied to a dynamical model of a hollow U-shaped tube.

2. Interval Field Concepts

2.1. General framework

Uncertain parameters in FE models typically have a spatial character: material properties such as density and Young's modulus or geometric properties such as plate thickness are geometrically oriented in space. In the context of dealing with uncertainty in simulation models, these parameters can show variability over the spatial domain, referred to as *geometric variability*. In FE-models, such a geometric parameter is discretised to the elements, leading to a set of discrete values representing that parameter in each element of the model. According to the possibility of geometric variability, the value in each element can vary separately, leading to different values in each element. However, some degree of dependency will usually be present and the value in different elements can not vary independently. Here the interval concept poses a problem. The uncertainty in each element could be captured by an interval parameter marking the bounds of the variation, but interval parameters are by definition incapable of incorporating the dependency present in the spatial domain. To mark the uncertainty present in such *field parameters* using a possiblistic technique, the *interval field* concept can be used. In its simplest form, an interval field consists of basis functions $\phi(\mathbf{r})$ representing the dependency and interval coefficients α^I representing the uncertainty. The explicit formulation of the interval field is defined as:

$$y^I(\mathbf{r}) = \sum_{i=1}^{n} \alpha^I \phi_i(\mathbf{r}) \tag{1}$$

with n the number of basis functions employed in the representation.

2.2. The Local Interval Field Decomposition method

2.2.1. *General objective*

For this interval field definition, we start from a field parameter $u(\mathbf{r})$, with $\mathbf{r}$ the spatial coordinates. When applied to an FE-model, such a continuous parameter is discretised to the elements of the FE-mesh, leading to a set of discrete parameters. Within this set a certain amount of spatial dependency is always present. The parameter value assigned to elements in close proximity to each other will show more interdependence than elements further away. This poses a problem for defining a plausible possibilistic field: the field can easily be made non-deterministic by defining an interval parameter in each element marking the bounds of the uncertain parameter value in each element, but this completely disregards any dependency present and will always overestimate the true uncertainty within such a parameter.

In probabilistic context, the Karhunen-Loeve expansion (Vanmarcke, 1993) provides an elegant solution to this by using the eigenvectors of the covariance matrix of the field as basis functions for a decomposition method. The coefficients that emerge can be proven to be uncorrelated and even independent in case of a Gaussian distribution. To define the entries of the covariance matrix, the correlation length of the field can prove a valuable parameter, defined in Eq. 2:

$$COV(x(\mathbf{r}_1), x(\mathbf{r}_2)) = \exp\left(\frac{\|\mathbf{r}_1 - \mathbf{r}_2\|}{L_\rho}\right) \tag{2}$$

In possibilistic context, correlation is not defined since it is related to the joint probability distribution functions which are not defined in this case. In the possibilistic case, we only consider (in)dependency of parameters, a much wider term than correlation. Since correlation is undefined, a new global dependency parameter has to be defined that is compatible with the possibilistic approach. The parameter that will be used in the method described in this section will be the *maximum gradient of the field parameter* (Imholz et al., 2015a; Imholz et al., 2016a). Intuitively, this makes sense if we define the dependency between two parameters as the maximum difference that can occur between the two parameters. E.g. , consider two parameters a and b, for which an intervals a^I and b^I of equal size are defined. If $a = b$ over the entire interval reach, the parameters are perfectly dependent, whereas in the opposite case, when the parameters can take values independently, the maximum difference is $\overline{a} - \underline{a}$. Now consider parameters a and b as instances of the same field parameter $u(\mathbf{r})$ at places in close proximity $\mathbf{r}_a$ and $\mathbf{r}_b = \mathbf{r}_a + d\mathbf{r}$. The case of perfect dependency then corresponds to a gradient equal to zero, whereas the case of perfect independency corresponds to a high maximum gradient, making this a valid parameter to represent the dependency.

The purpose of the interval field should be to accurately represent the true uncertain set, taking into account the possible dependency within the field. In the case of perfect dependency, a single discrete variable would suffise to represent the field variable in the entire domain. However, in every other case, each element of the discretised mesh can (at least partially) determine it's own value. The *dimensionality of the uncertainty therefore equals the total number of elements in the mesh*, regardless of the degree of dependency. To ensure the entire uncertain set is captured by the field, the *dimensionality of the interval field should be at least equal to the number of elements.*

As a conclusion, the interval field will should keep the dimensionality intact, but will transform the initial set of dependent interval parameters located in each element of the mesh, to a new set with *independent* parameters, *that will obey a priorly set condition on the maximum gradient in the field.*

2.2.2. *Mathematical definition*

The mathematical definition below follows the one explained in (Imholz et al., 2015a) for a field parameter in a one-dimensional space. The LIFD in 1D will write the non-determistic field $u(r)$ as an interval field $u^I(r)$ in the form of Eq. 1 that obeys the following statements:

1. $\forall \tilde{r} \in \Omega : U_{min} \leq u(\tilde{r}) \leq U_{max}$
2. $\forall r \in \Omega : \left| \frac{\partial u(r)}{\partial r} \right| \leq G_{max}$
3. $\forall \tilde{u}(r) : \overline{u} - \underline{u} \leq D_{max}$

The parameters G_{max}, U_{min}, U_{max} and D_{max} can be independently set. The first statement demands that the absolute bounds on the field parameter U_{min} and U_{max} are never exceeded. The second statement demands that the norm of the gradient never exceeds a preset value. This statement accounts for the dependency in the field. The third statement puts a bound on the difference between the maximal and minimal value of any realisation of the interval field. The objective of the LIFD is to obey the statements using the four governing uncertainty parameters mentioned above with an explicit interval field description with *independent* interval coefficients.

The only freedom we have is the shape of the basis functions. In the 1D-case, the basis functions have the following properties:

1. All ϕ_i are identically shaped radial basis functions.
2. A single ϕ_i is positioned at each element at location $\mathbf{r}_i$ of the FE mesh.
3. All ϕ_i are piecewise second order polynomial functions so the first derivatives are continuous.

figure 1 illustrates the shape of a basis function and its first derivative. To comply with all demands, the following explicit field is proposed:

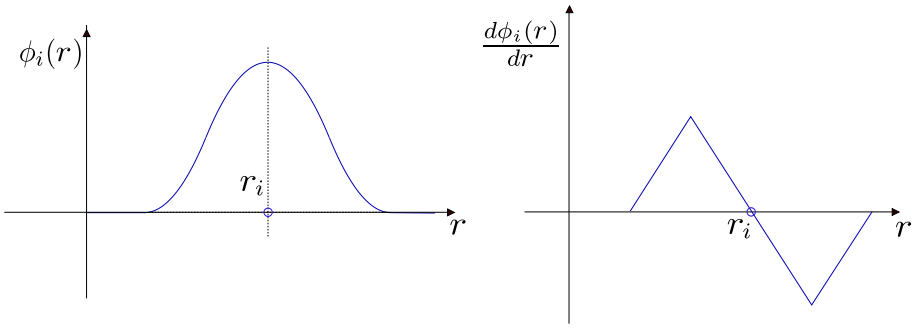

Figure 1. shape of a 1D radial basis function. Beyond a radius R from the center point, the basis function equals zero.

$$u^I(r) = C^I + \sum_{i=1}^{n} a \cdot 1_i^I \cdot \phi_i(r, R), \tag{3}$$

with $C^I = \langle \underline{C} | \overline{C} \rangle$ and $1_i^I = \langle 0|1 \rangle$ defined as the *unity* interval. The four controllable parameters are $\underline{C}$, $\overline{C}$, a and R. A unique mapping between these parameters and the four global uncertainty pararmeters is given by Eq. 4:

$$\begin{aligned} U_{max} &= \frac{a \cdot R}{dr} + \overline{C} \\ U_{min} &= \underline{C} \\ G_{max} &= \frac{a}{dr} \\ D_{max} &= \frac{a \cdot R}{dr} \end{aligned} \tag{4}$$

With dr the discretisation step of the mesh and R the effective radius of the basis functions. With these relations, the four global uncertainty parameters can be independently set, leading to a unique field definition as in Eq. 3.

2.2.3. *Adjustments*

For the purpose of dealing with bounded physical domains and local measurement data, a few adjustments can me made to the field mntionned above.

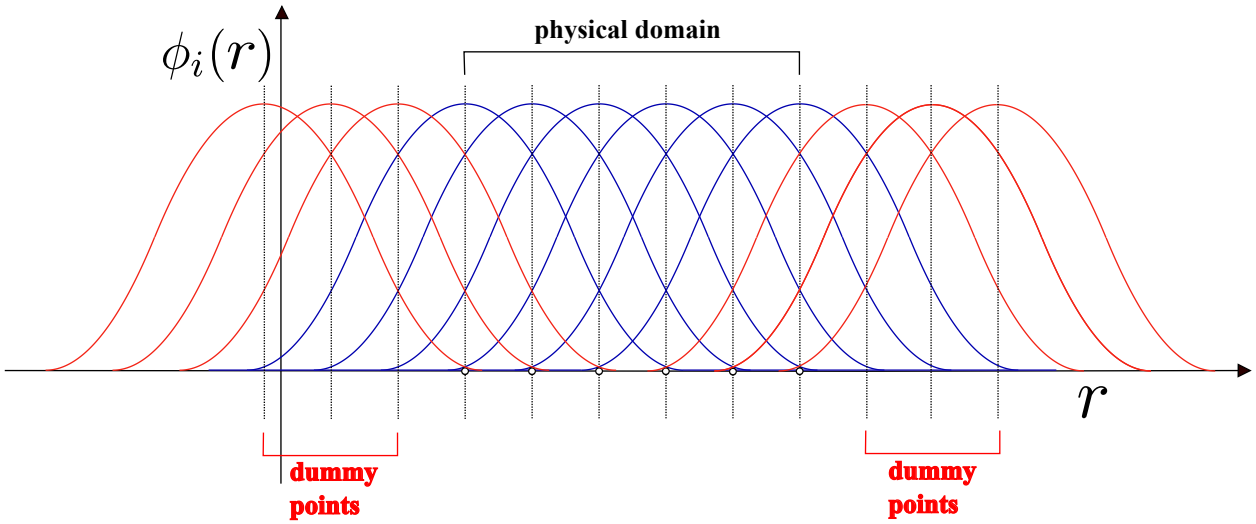

Figure 2. introduction of dummy points beoynd the physical domain in which non-physical basis functions are places, this to ensure the maximum gradient constraint is kept at the edges of the domain.

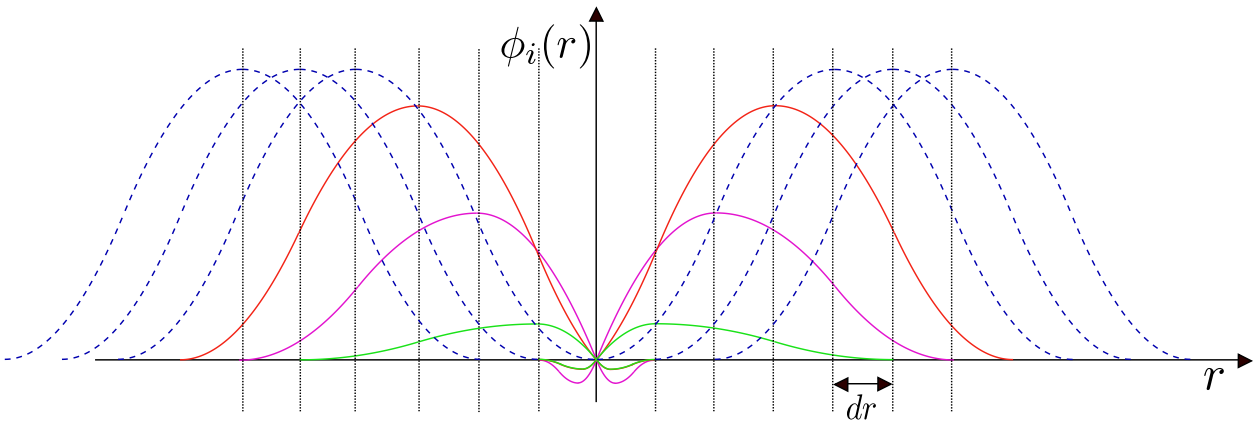

Figure 3. Adjustment of the basis function around a deterministic measurement point.

1. To ensure the maximum gradient constraint is kept over the entire domain, an adjustment is needed close to the edge of the domain. For points that lie within a distance R from a domain edge, the maximum constraint does not hold, because fewer basis functions have an effect in these points, leading to a smaller interval on the gradient in these points. To counter this, *dummy points* are added **beyond** the physical domain up to a distance R. The basis functions placed in these points lie partly in the physical domain and will ensure that the maximum

gradient constraint is kept over the entire physical domain. Figure 2 shows the dummy points beyond the physical domain.

2. Sometimes, local information can be available on the field parameter in a certain element, effectively fixing the value in that point. This limits the uncertain set to all realisations that smoothly run through this point. The shape function attached to this point is omitted, but to ensure the maximum gradient constraint is not violated, all base functions within a radius R of the point have to be adjusted as well. these adjustments are illustrated in figure 3.

2.3. Inverse Distance Weighting interpolation

Inverse Distance Weighting, as proposed by the authors in (De Mulder et al., 2012), constructs the base functions $\phi_i(\mathbf{r})$, needed for the explicit formulation of the Interval Field (1) based on the definition *a priori* selected locations $\mathbf{r}_i$ in the model geometry Ω. The selection of these locations $\mathbf{r}_i$ is based on the expert engineering knowledge of the analyst on where the uncertainty can be predicted within accurate bounds. The base functions are constructed following an inverse distance weighting, where it is assumed that the weight of an interval scalar α_i^I, defined at $\mathbf{r}_i$ decreases with the distance $\mathbf{r}$ from that respective location:

$$\phi_i(\mathbf{r}) = \frac{w_i(\mathbf{r})}{\sum_{j=1}^{n} w_j(\mathbf{r})} \tag{5}$$

,with n the number of base functions present in the interval field formulation. The weights $w_i(\mathbf{r})$ are calculated as the inverse of $d(\mathbf{r}_i, \mathbf{r})$ to the power of $p \in \mathbb{R}_{>0}$. $d(\mathbf{r}_i, \mathbf{r})$ is a distance measure between the location $\mathbf{r}_i$ where the interval is defined and the rest of the model $\mathbf{r}$. In the specific case of FE models, the concept of Euclidean distance is insufficient, as this yields non-physical paths between two points in the interpolation (De Mulder et al., 2012). It is therefore proposed to use a shortest path approach to calculate these distances.

An illustration of this concept is given in figure 4. The top graph of this figure shows all vertex realisations when three local intervals α_1^I, α_2^I and α_3^I are respectively defined at element 2, 4 and 8 in a 10 element 1D beam geometry, with $\alpha_1^I = [1.78; 1.85]$, $\alpha_2^I = [1.40; 1.75]$ and $\alpha_3^I = [1.3; 2.40]$. The middle graph shows the calculated weight functions $w_i(\mathbf{r})$ for the respective interval scalars and $p = 2$. Finally, the bottom graph shows the base functions $\phi_i(\mathbf{r})$ which are calculated based on the weighting functions for these locally defined interval scalars.

As can be noted, the locally defined intervals remain perfectly decoupled at the locations where they are defined, whereas the rest of the model can be seen as a weighted sum of their respective influences.

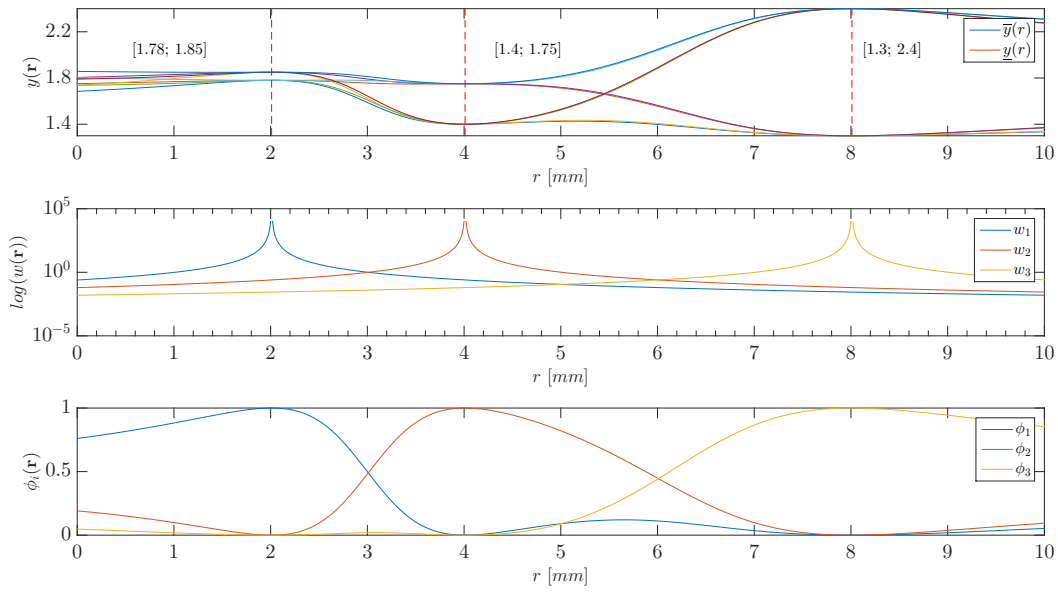

Figure 4. Illustration of the employed interpolation scheme. Top: vertex realisations of the resulting interval field, with the vertical lines indicating the locations of the interval scalars. Middle: Weight functions. Bottom: Base functions of the interval field, computed following Eq. 5.

3. Case Study

3.1. Object description and uncertainty definition

Both interval field formulations are applied to the dynamic analysis of a u-shaped tube. This tube is produced following a cold-forming process and hence the largest uncertainty is located in the bent part. Therefore, only this part is considered as uncertain in the following analysis. An illustration of this model is shown in figure 5. An FE model of this geometry is constructed using 75 beam elements and the model is solved for the first ten non-rigid eigenfrequencies.

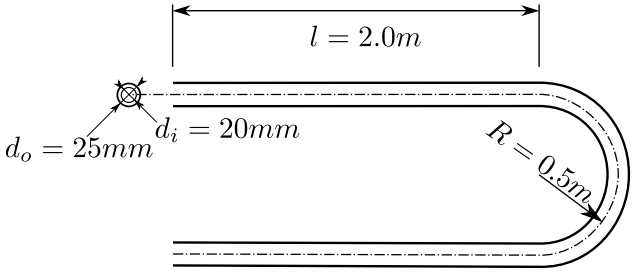

Figure 5. Illustration of the geometry of the u-shaped cold formed beam under consideration.

We assume the E-modulus of the tube is subject to uncertainty, ultimately limited to ±55% of the nominal value. The uncertain part of the tube is limited to the curved part, the straight ends are assumed to be deterministic. In the curved part, the two methods mentioned above are used to create an interval field for the 21 elements located there.

1. An interval field is defined by imposing that the interval scalars at elements 33 and 43 are both defined as $[93.12 \cdot 10^{09}\ Pa;\ 320.8 \cdot 10^{09}\ Pa]$ and is constructed following the IDW technique. Only the uncertainty between element 28 and 48 is regarded in the analysis. C_0 continuity in the realisations of Young's Modulus at the border between the *certain* and *uncertain* region is guaranteed by imposing infinitely thin intervals at elements 28 and 48. Propagation of the IDW interval field is performed following the vertex method (Dong and Shah, 1987). A maximum gradient of $5 \cdot 10^{05}\ MPa/m$ is thus obtained in the realisations of the IDW interval field. The interval field and its gradients for this model is shown in figure 6.

2. For the LIFD, an R-value equal to 0.3m (4 element-lengths) and a-value equal to $40 \cdot 10^3$ MPa provide limits that are similar to the IDW case. In the endpoints of the curved part, measurement points are introduced to fix the field there at the nominal value. This leads to an interval field description with 21 terms, one interval parameter and corresponding shape function in each element. Some realisations are given in figure 7. To propagate this field, a response surface is created using *coefficient fields*. Basically, this is a polynomial model that takes into account the dependency between E-moduli in adjacent elements by assuming the coefficients of the polynomial are continuous functions of the spatial coordinate r as well (Imholz et al., 2016a).

Obviously, the analysis using IDW is much more straightforward to perform and less time-consuming, as it only uses two uncertain independent variables. The LIFD attempts to capture the entire set of realisations that obey the maximum gradient constraint using 21 uncertain independent variables, at the cost of increased computational work. The uncertain set of the IDW is a subset of the uncertain set of the LIFD, which is realised by keeping the maximum derivative and maximum deviation equal between both approaches. As a result, the uncertain output set of eigenfrequencies obtained with IDW should be a subset of the uncertain output set obtained with LIFD.

3.2. RESULTING UNCERTAINTY ON THE EIGENFREQUENCIES

In both cases, the uncertain domain at the output is a region within a ten-dimensional domain containing the 10 eigenfrequencies. To allow for graphical verification, this domain is projected on some two-dimensional subdomains considering only two eigenfrequencies. Figure 8 shows the result of the vertex method computation for the IDW interval field. ω_m in this figure denotes one realisation of the input interval field, while C_m indicates the convex hull of the uncertainty region spanned by these realisations, as proposed by the authors in (Faes et al., 2016a; Faes et al., 2016b). Two vertex realisations ($[\underline{E};\overline{E}]$ and $[\overline{E};\underline{E}]$) of the IDW interval field are coincident due to the symmetry of both the IWD interval field and the model geometry, leading to a triangular uncertainty region in 10 dimensions.

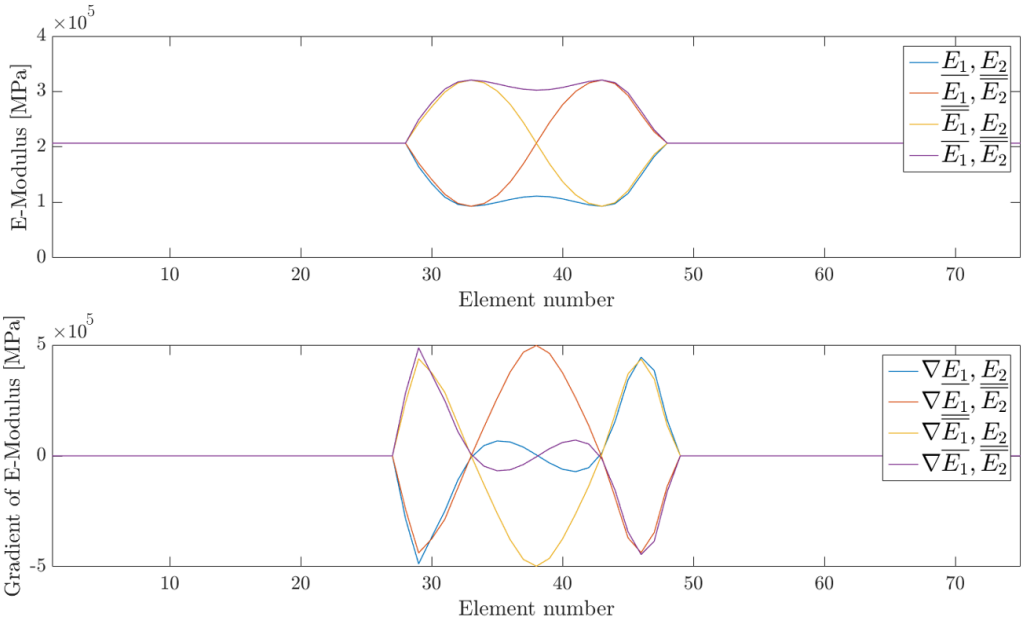

Figure 6. Top: Vertex realisations of the interval field obtained by regarding the spatial uncertainty between elements 28 and 48, obtained by interpolating $[93.12 \cdot 10^{09};\ 320.8 \cdot 10^{09}]$ and $[93.12 \cdot 10^{09};\ 320.8 \cdot 10^{09}]$ at elements 33 and 43. Bottom: gradients of the vertex realisations of the interval field.

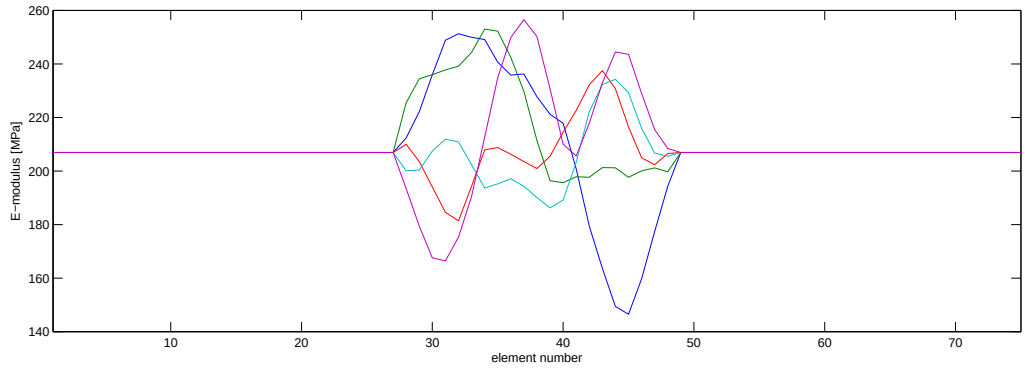

Figure 7. Some configurations generated by using the LIFD method.

For the LIFD, the vertex method is not applicable as the relatively large amount of variables (= 21) already amounts to over two million vertex points. Instead, a tracking algorithm was introduced by the authors in (Imholz et al., 2016b) that creates the 2D-projections of uncertain regions originating from *monotonous* problems directly. Starting in the minimum vertex point, where all inputs are at their minimal value, The upper bound curve is found by setting steps along a path that attempts to maximize the quantity $\frac{\partial \omega_y}{\partial E_i} / \frac{\partial \omega_y}{\partial E_i}$, whereas the lower bound curve is found

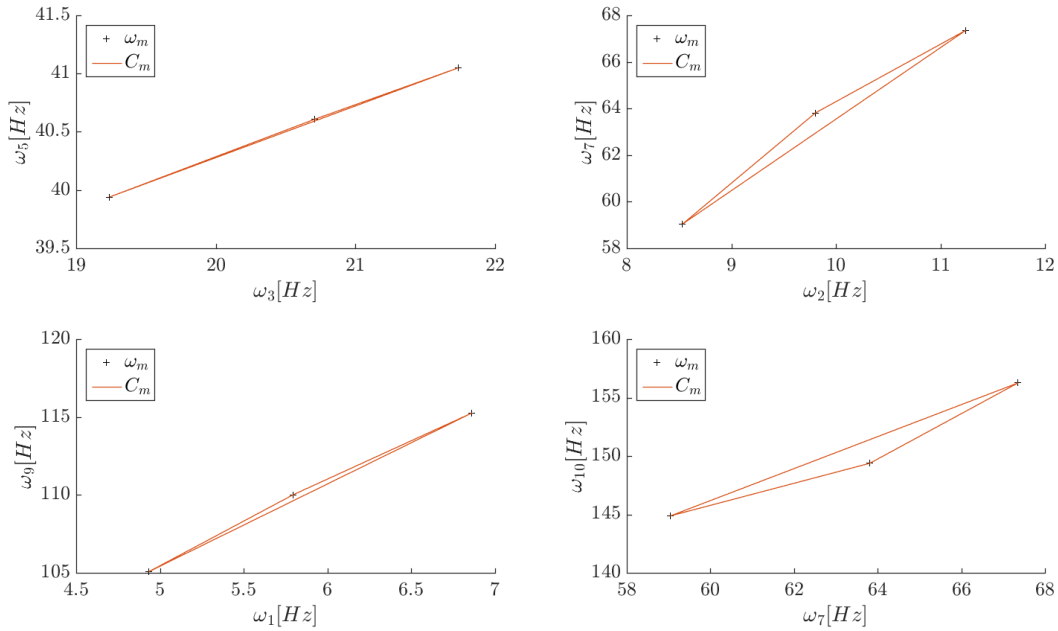

Figure 8. Two dimensional subdomains of the ten dimensional output space, obtained by performing the vertex method on the IDW interval field.

by setting steps along a path that attempts to minimize it. This approach is especially suited for identifying 'shuttle'-shaped uncertain regions, which are common for monotonous I/O-relations.

3.3. Observations

Figure 9 again shows the uncertain regions obtained from the IDW case, but the figure is expanded with the results of the LIFD-analysis. In this figure, the shuttle shapes can be seen very clearly. Our initial requirement that the IDW region should be a subset of the LIFD-region seems to be met. The uncertain region obtained from the LIFD is clearly much 'wider', indicating a less pronounced dependency between eigenfrequencies in the mid-vertex region (= half-way between the corner points). It is interesting to take a look at which realisations are responsible for this observation. If we look at the plot concerning ω_3 and ω_5, we are specifically interested in the point P, located on the upper bound curve. Figure 10 shows the input realisation that corresponds to this point. From the shape, we can see that IDW using only 2 uncertain parameters at the locations mentioned does not include this configuration in its uncertain set, and therefore it is not propagated to the output. Putting in an extra uncertain parameter in the middle in-between the two current parameters would solve this problem. However, the possibility remains that critical configurations in other frequency pairs remain neglected. Because LIFD takes into account all possible configurations bounded by the maximum gradient constraint, the LIFD-approach does not suffer from this problem. However, the increased dimensionality brings along problems of its own, leading to increased computational

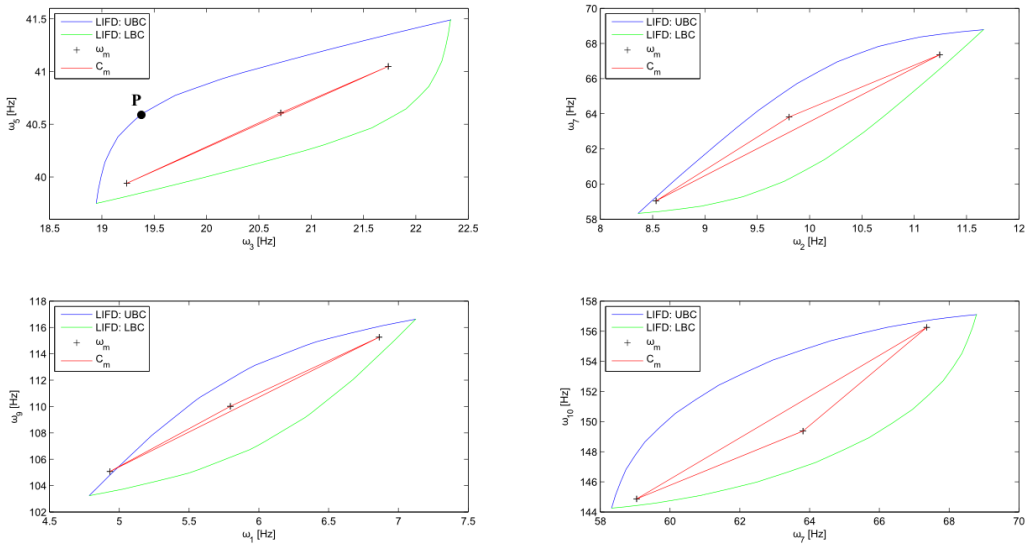

Figure 9. Two dimensional subdomains of the ten dimensional output space, both for the IDW and LIFD method. Upper left: frequency 3 and 5, upper right: frequency 2 and 7, lower left: frequency 2 and 9, lower right: frequency 7 and 10. UBC = upper bound curve, LBC = lower bound curve.

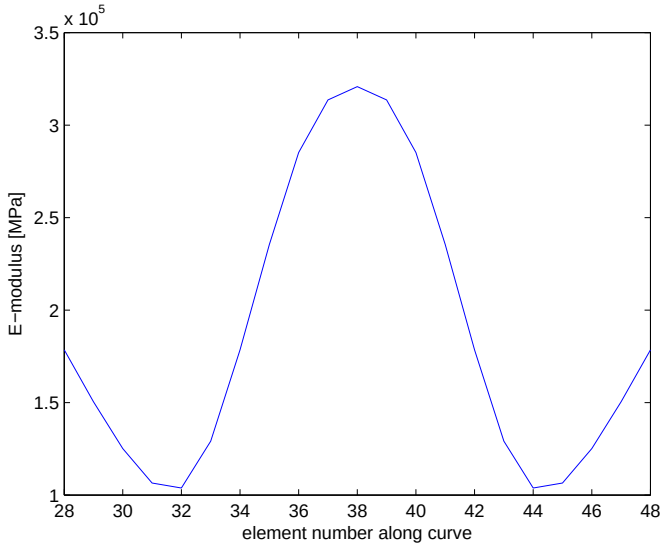

Figure 10. Realisation corresponding to the point P indicated in Figure 9.

work. The vertex method used by IDW only requires four FE-model evaluations (Actually only three, because two vertices are equal due to symmetry of the tube). The response surface used by

LIFD was build upon a sample set of 50 samples, after which the remaining work to compute the uncertain regions was neglectible. The efficient use of the coefficient functions prevents us from increasing the problem dimension to infeasible heights.

4. Conclusions

The importance of Uncertainty Quantification for the purpose of creating relaible designs cannot be stretched enough. This paper elaborated and compared two types of possiblistic uncertainty modelling using the interval as basic tool to represent non-deterministic parameters. Essentially, the concept of interval fields extend the use of intervals to geometric parameters by taking into acount possible spatial dependence within such a field. The two concept described here both approach the problem in a different manner: the IDW-method requires a preliminary choice of the locations where independent interval parameters will be placed in space, and then interpolates to all other points in the field. The LIFD starts from a global uncertainty definition by setting bounds on the maximum derivative and converts this to an interval field that puts an independent interval parameter in each point of the FE-mesh the field is defined on, thereby ensuring the entire uncertain set is captured at the cost of high dimensionality. As a final conclusion, one can say that IDW works well in problems were the sensitive points in the spatial domain are known beforehand and the number of output parameters is limited, since the sensitive points may vary for each output parameter. When multiple output parameters are considered, the LIFD provides a more robust approach to find the complete uncertain output set for a certain minimal gradient constraint.

References

De Mulder, W., D. Moens, D. Vandepitte. Modeling Uncertainty in the Context of Finite Element Models With Distance-Based Interpolation, in: Uncertainties 2012, Sao Paulo, Brazil, 2012.

Dong, W. and H. C. Shah. Vertex Method for Computing of Fuzzy Variables, Fuzzy Sets Systems, 24:65–78, 1987.

Faes, M., J. Cerneels, D. Vandepitte and D. Moens. Identification of Interval fields for spatial uncertainty representation in Finite Element models. Proceedings of the European Congress on Computational Methods in Applied Sciences and Engineering. Hersonissos, Greece, 5-10 June 2016.

Faes, M., J. Cerneels, D. Vandepitte and D. Moens. A convex set-based optimization scheme for the identification of Interval Field uncertainty in Finite Element models. Joint Annual Meeting of DMV and GAMM. Braunschweig, Germany, 7 - 11 March 2016.

Imholz, M., D. Vandepitte and D. Moens. Derivation of an input interval field decomposition based on expert knowledge using locally defined basis functions, proceedings of the 1st International Conference on Uncertainty Quantification in Computational Sciences and Engineering, Hersonissos, Greece, September 2015.

Imholz, M., D. Vandepitte and D. Moens. Analysis of the effect of uncertain clamping stiffness on the dynamical behaviour of structures using interval field methods, proceedings of ICUME 2015, Darmstadt, Germany, November 2015.

Imholz, M., D. Vandepitte and D. Moens. Application of interval fields to geometric output quantities of Finite Element models, proceedings of UNCERTAINTIES2016, Maresias, Brazil, February 216.

Imholz, M., D. Vandepitte and D. Moens. Dynamical analysis of plate models with uncertain structural properties using the interval field method, proceedings of ECCOMAS 2016, Hersonissos, Greece, June 2016.

Vanmarcke, E., Random Fields: analysis and synthesis, MIT Press, Cambridge, 1993.